ISSN 1995-0802, Lobachevskii Journal of Mathematics, 2021, Vol. 42, No. 14, pp. 3486–3496. © Pleiades Publishing, Ltd., 2021.

Bistability in a One-Dimensional Model of a Two-Predators-One-Prey Population Dynamics System

S. Kryzhevich[1,2,3*], V. Avrutin[4], and G. Söderbacka[5***]**

(Submitted by S. Yu. Pilyugin)

[1] *Institute of Applied Mathematics, Faculty of Applied Physics and Mathematics, Gdańsk University of Technology, Gdańsk, 80-233 Poland*

[2] *BioTechMed Center, Gdańsk University of Technology, Gdańsk, 80-233 Poland*

[3] *St. Petersburg State University, St. Petersburg, 199178 Russia*

[4] *Institute for Systems Theory and Automatic Control, University of Stuttgart, Stuttgart, 70569 Germany*

[5] *Åbo Akademi, Turku, FI-20500 Finland*

Received July 25, 2021; revised August 30, 2021; accepted September 4, 2021

Abstract—In this paper, we study a classical two-predators-one-prey model. The classical model described by a system of three ordinary differential equations can be reduced to a one-dimensional bimodal map. We prove that this map has at most two stable periodic orbits. Besides, we describe the bifurcation structure of the map. Finally, we describe a mechanism that leads to bistable regimes. Taking this mechanism into account, one can easily detect parameter regions where cycles with arbitrary high periods or chaotic attractors with arbitrary high numbers of bands coexist pairwise.

DOI: 10.1134/S1995080222020135

Keywords and phrases: *population dynamics, two-predators-one-prey model, bimodal smooth maps, Schwarzian derivative, period doubling bifurcations, bistability.*

1. INTRODUCTION

Modeling ecosystems is one of the well-established parts of the theory of dynamical systems. One of the standard models in this area is the Lotka–Volterra system, also known as the prey-predator model. The behavior of this two-dimensional autonomous system of differential equations is well known: the system may exhibit stationary or periodic solutions only.

Conversely, ecological models involving competition between two or more predators (and, possibly, more species of prey) may demonstrate a sophisticated behavior, including chaotic dynamics. Besides, the number of attracting sets (periodic or chaotic) may vary.

The general case of a two-predators-one-prey system is considered by Hsu, Hubell, and Waltman in [15–17]. The models considered in the cited works are based on ecological laws described initially by Holling in [14]. A good review of recent results in population dynamics can be found in [6].

A study of periodic solutions of the above-mentioned models together with a detailed bifurcation analysis is presented in [4, 18] and [26]. Two-dimensional and three-dimensional models in discrete time and the bifurcations of their equilibria are considered in [29].

A model with additional terms responsible for competition between predators is studied in [24]. Extinction conditions are discussed for predator species, stability of fixed points and other invariant sets is analyzed.

*E-mail: kryzhevicz@gmail.com
**E-mail: viktor.avrutin@ist.uni-stuttgart.de
***E-mail: gsoderba@abo.fi

A model with ratio-depending predator growth rates is introduced in [7]. Equilibrium analysis is performed, and extinction conditions for predators are presented. Various generalizations of the Lotka–Volterra model with polynomials at the right-hand side have also been studied, see, for example, [13] and [23]. More sophisticated models including stochastic terms [10, 19] or taking into account diffusion phenomena [20] are also developed.

In the present work, we consider a classical two-predators-one-prey model. Following [27], this model can be approximated by a one-dimensional bimodal map. Previously, it has been observed that typically this map has a unique attractor, although for some parameter values it also may exhibit bistability (coexistence of two attractors). The goal of the present paper is to describe the mechanism leading to this effect.

The paper is organized as follows.

In Sec. 2 and Sec. 3, the considered 3D model in continuous time and its one-dimensional approximation in discrete time are introduced, respectively. For the one-dimensional map, we apply the classical techniques developed by Devaney and demonstrate that this map cannot have more than two attractors. Thereafter, in Sec. 4 we identify the regions in the parameter space where bistability occurs. We demonstrate that this kind of dynamics occurs in neighborhoods of the intersection points of bifurcation curves forming so-called shrimp-structures.

2. TWO-PREDATORS-ONE-PREY MODEL

Let us consider the two-predators-one-prey model given by the following three differential equations

$$\begin{aligned} \dot{X}_i &= p_i\varphi_i(S)X_i - d_iX_i, \quad i = 1, 2; \\ \dot{S} &= H(S) - q_1\varphi_1(S)X_1 - q_2\varphi_2(S)X_2 \end{aligned} \tag{1}$$

investigated previously in [27]. Here, the non-negative values S and X_i, $i = 1, 2$, represent quantities of the prey and predators respectively; H and φ_i are smooth functions with $H(0) = 0$, H being of the logistic type and both functions φ_i being non-decreasing. Parameters p_i, d_i and q_i are positive. Using the normalized variables $s = \frac{S}{K}$, $\quad y_i = \frac{q_iX_i}{rK}, i = 1, 2$, Eqs. (1) can be rewritten as

$$\begin{aligned} \dot{y}_i &= \phi_i(s)y_i, \quad i = 1, 2; \\ \dot{s} &= h(s) - \psi_1(s)y_1 - \psi_2(s)y_2, \end{aligned} \tag{2}$$

where

$$h(s) = \frac{1}{K}H(sK), \quad \psi_i(s) = \varphi_i(sK), \quad \phi_i(s) = p_i\psi_i(s) - d_i.$$

In this paper, we choose the functions $\phi_i(s)$, $h(s)$, and $\psi_i(s)$ to be defined as follows:

$$\phi_i(s) = m_i\frac{s - \lambda_i}{s + a_i}, \quad \psi_i(s) = \frac{s}{s + a_i}, \quad i = 1, 2; \quad h(s) = (1 - s)s,$$

where a_1, a_2, λ_1 and λ_2 are positive. Then, system (2) takes the following form:

$$\begin{aligned} \dot{y}_i &= m_i\frac{s - \lambda_i}{s + a_i}y_i, \quad i = 1, 2, \\ \dot{s} &= \left(1 - s - \frac{y_1}{s + a_1} - \frac{y_2}{s + a_2}\right)s. \end{aligned} \tag{3}$$

Dissipativity of this system and the extinction conditions for one of the predators are considered in [27] (see also [1]). There, possible equilibria of this system are studied as well as some periodic solutions. In particular, it is shown in the cited work that there are no stationary solutions related to the coexistence of predators for $\lambda_1 \neq \lambda_2$ or $a_1 \neq a_2$ and that the coexistence of periodic or chaotic solutions is possible.

The structure of Poincaré maps corresponding to the condition $s = \text{const}$, $\dot{s} < 0$ near fixed points is studied in [21]. It is shown in [8] and [9] that for a broad range of parameter values the considered system

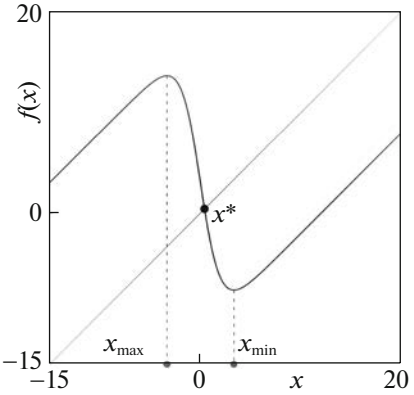

Fig. 1. Graph of the one-dimensional map (5), $b = -12$, $k = -30$. Colored versions of all the figures are available at arxiv.org/pdf/2108.06739.pdf.

exhibits a strong contraction in the $(y_1 + y_2)$-direction in which case its dynamics can be approximated by the one-dimensional map given by

$$x_{n+1} = f(x_n) = \beta + x_n - \frac{k_1 + k_2 e^{x_n}}{1 + e^{x_n}} u, \tag{4}$$

where β, u and k_i are parameters. Here $x_j = \log(y_{2j}/y_{1j})$, where y_{1j} and y_{2j} are values of y_1 and y_2 respectively calculated in the jth step.

Remark 1. Note that for parameter values which do not lead to a strong contraction in the $(y_1 + y_2)$-direction, system (3) cannot be described by a one-dimensional map and presumably may exhibit such phenomena as Shil'nikov's spiral chaos and coexistence of at least three attractors (see [3, 21, 27]). As discussed below, this cannot occur in the one-dimensional model (4).

3. ONE-DIMENSIONAL MODEL AND ITS PROPERTIES

It can easily be shown that map (4) can be written in the following form

$$x_{n+1} = f(x_n) = b + x_n - \frac{k}{1 + e^{x_n}}, \tag{5}$$

where $b = \beta + k_2 u$, $k = (k_1 - k_2)u$. An example of the graph of the function f in Eq. (5) is shown in Fig. 1. In the following we consider the dynamics of map (5) in the parameter domain

$$P = \{(b, k) \mid k < b < 0\} \tag{6}$$

as outside this domain all trajectories either diverge or converge to a stable fixed point.

Remark 2. The map has the following symmetry property

$$f(x)|_{b=b^*,k=k^*} = -f(-x)|_{b=k^*-b^*,k=k^*}\,.$$

Therefore, if the map at the parameter values $b = b^*$, $k = k^*$ has a period-n orbit $\{x_1, \ldots, x_n\}$, then the map at the parameter values $b = k^* - b^*$, $k = k^*$ has the period-n orbit $\{-x_1, \ldots, -x_n\}$. As a consequence, the bifurcation structures of the map in the parameter regions

$$P_1 = \{(b, k) \mid 2\,b < k < b < 0\} \quad \text{and} \quad P_2 = \{(b, k) \mid k \le 2\,b < 0\}$$

with $P = P_1 \cup P_2$ (see Fig. 2) are topologically equivalent.

1. The fixed point and the period-2 orbit. Note that for $k \ge -4$ the function f has a local minimum and a local maximum at the points

$$x_{\max} = \ln\left(-1 - \tfrac{1}{2}k - \tfrac{1}{2}\sqrt{4k + k^2}\right), \quad x_{\min} = \ln\left(-1 - \tfrac{1}{2}k + \tfrac{1}{2}\sqrt{4k + k^2}\right)$$

respectively. Evidently, $x_{\min} = -x_{\max} > 0$. The map is increasing for $x < x_{\max}$ and for $x > x_{\min}$ and decreasing in the interval $\{x_{\max}, x_{\min}\}$ containing the unique fixed point of the map $x^* = \ln\left(\frac{k}{b} - 1\right.$

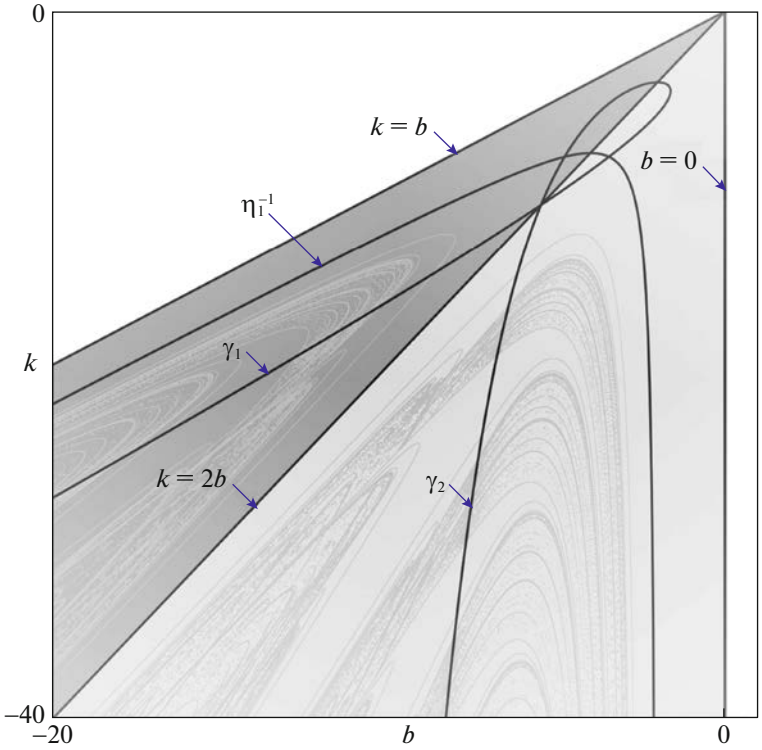

Fig. 2. Boundaries of the regions P, P_1, P_2, $P^s_{x^*}$ in the parameter space and the boundaries of the regions corresponding to different definitions of the globally attracting absorbing intervals. Additionally, the bifurcation structure calculated numerically is shown (see also Fig. 4). The regions P_1 and P_2 are highlighted in dark and light grey, respectively.

existing for $(b, k) \in P$. As the parameter values approach the boundaries of P, the fixed point tends to $\pm\infty$ (i.e., for a fixed value of $k < 0$, if $b \to k$ from the right and $x^* \to \infty$ if $b \to 0$ from the left).

From the condition $f'(x^*) > -1$, we obtain that the fixed point is attracting (moreover, it is globally attracting) in the parameter region

$$P^s_{x^*} = \quad (b, k) \in P \mid k > \frac{b^2}{b+2}, \quad b > -2 \quad .$$

At the boundary of the region $P^s_{x^*}$, i.e., at the curve

$$\eta_1^{-1} = \quad (b, k) \in P \mid k = \frac{b^2}{b+2}, \quad b > -2$$

the fixed point x^* undergoes a supercritical period-doubling bifurcation leading to the appearance of a period-2 orbit. As shown by the following lemma, this period-2 orbit exists in the complete parameter region $P \setminus P^s_{x^*}$:

Lemma 1. *For any (b, k) such that $k < \frac{b^2}{b+2}$, $b < -2$, the map (5) has a period-2 orbit.*

Proof. Evidently, $\lim_{x\to-\infty} f(x) - x = b - k$, $\lim_{x\to\infty} f(x) - x = b$. Consequently,

$$\lim_{x\to-\infty} f^2(x) - x = 2(b-k) > 0, \quad \lim_{x\to\infty} f^2(x) - x = 2b < 0.$$

On the other hand, $(f^2)'(x^*) = (f'(x^*))^2 > 1$. Therefore, the equation $f^2(x) - x = 0$ has at least one solution in the interval $(-\infty, x^*)$ and another one in the interval (x^*, ∞). The fixed point x^* is unique, so these solutions correspond to a period-2 orbit. □

Moreover, one can actually prove a more general result:

Lemma 2. *For any (b, k) such that $k < \frac{b^2}{b+2}$, $b < -2$, at least one of the following statements applies:*

1. *There exists an $n \in \mathbb{N}$ such that map (5) has a stable period-2^n orbit.*

2. *The map has period-2^n orbits for all $n \in \mathbb{N}$.*

The proof of this lemma is similar to that of Lemma 1.

Lemma 1 proves the existence of at least one period-2 orbit. However, for each $b \in (P \setminus P^s_{x^*})$ there exists only one period-2 orbit. This is shown in Lemma 3.

Lemma 3. *For any (b, k) such that $k < \frac{b^2}{b+2}$, $b < -2$, map (5) can have at most one period-2 orbit.*

Proof. The idea of the proof is as follows. Given a period-2 orbit $\{x_1, x_2\}$, $x_2 > x_1$ of map (5), we express k and b as functions of x_1 and x_2. Then we consider values k and b such that $B := 2\,b/k = \text{const}$, and represent k as a function of x_1. We show that the latter function is strictly monotone which implies that two distinct orbits $\{x_1, x_2\}$ cannot correspond to a pair (k, b).

$$B = u_1 + u_2, \quad k = \frac{2\,(x_2 - x_1)}{u_2 - u_1}, \quad \text{where} \quad u_i = \frac{1}{1 + e^{x_i}}, \quad i = 1, 2. \tag{7}$$

Note that $0 < u_i < 1$ and $u_2 < u_1$ implying $u_1 > B/2$. From $k < b < 0$ follows $0 < B < 2$. Thus $B/2 < u_1 < B$ if $B < 1$ and $B/2 < u_1 < 1$ if $B \geq 1$. Solving the last equality of (7) for x_i, we get $x_i = \ln\left(\frac{1}{u_i} - 1\right) = h(u_i)$. Henceforth, we drop the subscript and write u instead of u_1. So, we can express k as a function of u:

$$k(u) = \frac{2(h(u) - h(B - u))}{2u - B}.$$

Since $h'(u) = 1/[u(u-1)]$ we obtain

$$\lim_{u \to B/2} k(u) = 2\,h'(B/2) = \frac{8}{B\,(B-2)}, \tag{8}$$

where the limit is taken from the right side. Moreover, it follows by the Lagrange theorem that $k < 2 \max h'(u) = h'(B/2) = \frac{8}{B\,(B-2)}$. The function $h'(u)$ is convex for $u \in (0, 1)$ and, consequently

$$h'(B - u) + h'(u) < 2h'(B/2) = \frac{8}{B\,(B-2)}$$

for any $u \in (B/2, \min(B, 1))$.

Now we calculate the derivative of k:

$$k'(u) = \frac{2}{2u - B}\left(h'(B - u) + h'(u) - k \;\; < \frac{2}{B - 2u}\left(\frac{8}{B\,(B-2)} - k\right)\right.$$

for any $u > B/2$. So, taking into account the initial conditions (8), we obtain that

$$k(u) < \frac{8}{B\,(B-2)}$$

and, moreover, $k'_u(u) < 0$ for any $u > B/2$. This implies the uniqueness of the period-2 orbit. □

Remark 3. Orbits (even stable ones) of periods higher than 2 may be non-unique. One can find numerically that two period-4 attractors can coexist (e.g. for $b = -7.55$ and $k = -19.06$).

2. A globally attracting interval. It is easy to see that for $(b, k) \in P$ the function f satisfies $f(x) > x$ for $x < x^*$ and $f(x) < x$ for $x > x^*$. Therefore, either the fixed point is globally attracting or there map has a globally attracting absorbing interval around x^*. The boundaries of this interval are given by the images of the points $x_{\max}$ and $x_{\min}$, as illustrated in Fig. 3. As one can see, in the left part of this figure the absorbing interval is given by $[f^2(x_{\max}), f(x_{\max})]$, in the middle part by $[f(x_{\min}), f(x_{\max})]$, and in the right part by $[f(x_{\min}), f^2(x_{\min})]$. As shown below in Lemma 4, the regions in the parameter space corresponding to these configurations are separated from each other by the curves

$$\gamma_1 = \{(b, k) \in P \mid f(x_{\max}) = x_{\min}\} = \{(b, k) \in P \mid b = b_1\},$$

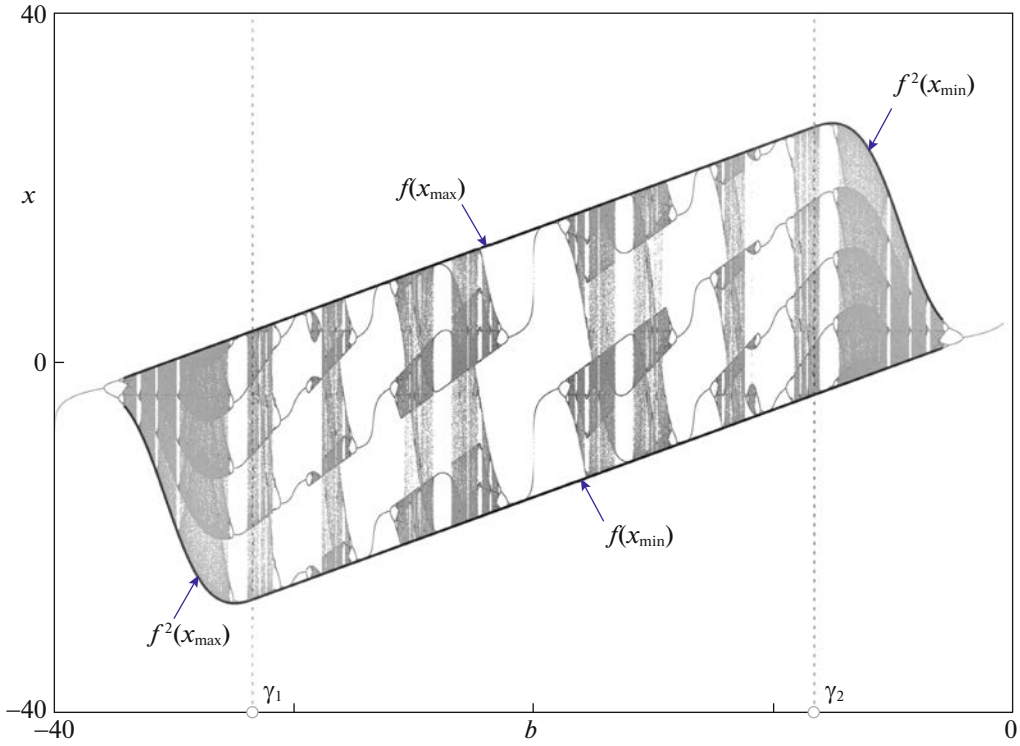

Fig. 3. Bifurcation sequence at $k = -40$. Boundaries of the globally attracting absorbing intervals are indicated.

$$b_1 = 2\,x_{\min} - 1 - e^{x_{\min}}, \quad b_2 = 2\ln\left(-1 - \tfrac{1}{2}k + \tfrac{1}{2}\sqrt{4k + k^2}\right) + \tfrac{1}{2}k - \tfrac{1}{2}\sqrt{4k + k^2};$$
$$\gamma_2 = \{(b,k) \in P \mid f(x_{\min}) = x_{\max}\} = \{(b,k) \in P \mid b = b_2\},$$
$$b_2 = -2\,x_{\min} - 1 - e^{-x_{\min}} = 2\ln\left(-1 - \tfrac{1}{2}k - \tfrac{1}{2}\sqrt{4k + k^2}\right) + \tfrac{1}{2}k + \tfrac{1}{2}\sqrt{4k + k^2}$$

(see Fig. 2 for graphs of γ_1 and γ_2). Using this notation, we can state the following

Lemma 4.

1. *If $b < \min(b_1, b_2)$ then the interval $J_- = \{(f^2(x_{\max}),\ f(x_{\max})\}$ does not contain $x_{\min}$ and is globally attracting.*

2. *If $b > \max(b_1, b_2)$ then the interval $J_+ = \{(f(x_{\min}),\ f^2(x_{\min})\}$ does not contain $x_{\max}$ and is globally attracting.*

3. *If $b_2 < b < b_1$ then the interval $\{(f(x_{\min}),\ f(x_{\max})\}$ does not contain any of $x_{\min}$ and $x_{\max}$. In this case, the function f is monotonous on this interval. Therefore, the function cannot have any invariant sets different from a fixed point and a period-2 orbit.*

4. *If $b_1 < b < b_2$ then the interval $J_0 = \{(f(x_{\min}),\ f(x_{\max})\}$ contains both $x_{\min}$ and $x_{\max}$ and is globally attracting.*

The proof of this lemma follows from the definitions of b_1 and b_2.

Note that the absorbing intervals J_-, J_+ and J_0 in cases 1, 2 and 4 respectively are positively invariant.

However, if $b_2 < b < b_1$, the fixed point and the period-2 orbit cannot be stable at the same parameter value. Hence, in this case, there is only one stable periodic orbit.

Calculating the Schwarzian derivative for the map (5), we get

$$S\,f(x) = k\,e^x\,\frac{2(e^x - 1)^2 - (k+4)\,e^x}{2((e^x+1)^2 + k\,e^x)^2}$$

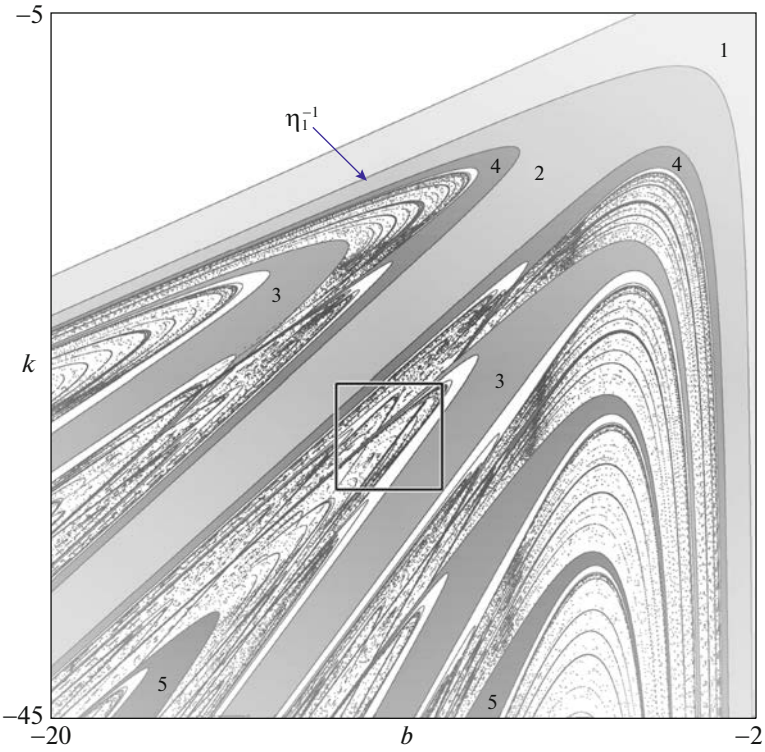

Fig. 4. Regions of the parameter plane corresponding to different periods of stable orbits.

which is negative for $k < -4$.

Let $b < \min(b_1, b_2)$. Then the positively invariant and globally attracting absorbing interval $J_- = [f^2(x_{\max}), f(x_{\max})]$ contains the point $x_{\max}$ and does not contain $x_{\min}$. In other words, the map is unimodal on J_-. It follows from the classical result of Devaney [5, Theorem 11.4] that in this case any stable periodic orbit (and, in fact, any attractor) attracts $x_{\min}$. So, such an orbit is necessarily unique. The case $b \geq \max(b_1, b_2)$ is similar. Therefore, the dynamics of the map for parameter values inside the region P but outside the region between the curves γ_1, γ_2 below their intersection point (see Fig. 2) cannot be affected by bistability.

Finally, if $b_1 < b < b_2$, the globally attracting positively invariant absorbing interval J_0 contains both $x_{\min}$ and $x_{\max}$. Therefore, as follows from the Devaney's result mentioned above, it can contain two attractors, with $x_{\min}$ belonging to the basin of one of them, and $x_{\min}$ to the basin of other one. Accordingly, the map in the parameter region shown in Fig. 2 between the curves γ_1, γ_2 below their intersection point can exhibit bistability.

4. PERIOD DOUBLING CASCADES AND COEXISTING PERIODIC SOLUTIONS OF DISTINCT PERIODS

In order to explain the occurrence of bistability in map (5) in the parameter region between the curves γ_1, γ_2, let us consider the complete bifurcation structure in the 2D parameter space (b, k). Fig. 4 shows this structure including regions corresponding to stable cycles of higher periods calculated numerically. As illustrated in the magnification of this structure shown in Fig. 5, in the parameter domain P given by Eq. (6) the bifurcation curves form so-called *shrimp*-structures [12], previously observed in several one-dimensional and two-dimensional maps [22, 28], including the well-known Hénon map. For a detailed description of the "anatomy" of a shrimp-structure, we refer to [11].

A distinguishing feature of the shrimp-structures is the presence of the so-called "tails", i.e., long and narrow parameter regions confined from one side by a fold (saddle-node) bifurcation curve issuing from the central part of the structure and approaching infinity. Inside these narrow regions, one observes a complete period-doubling cascade and thereafter by the complete logistic map scenario, including

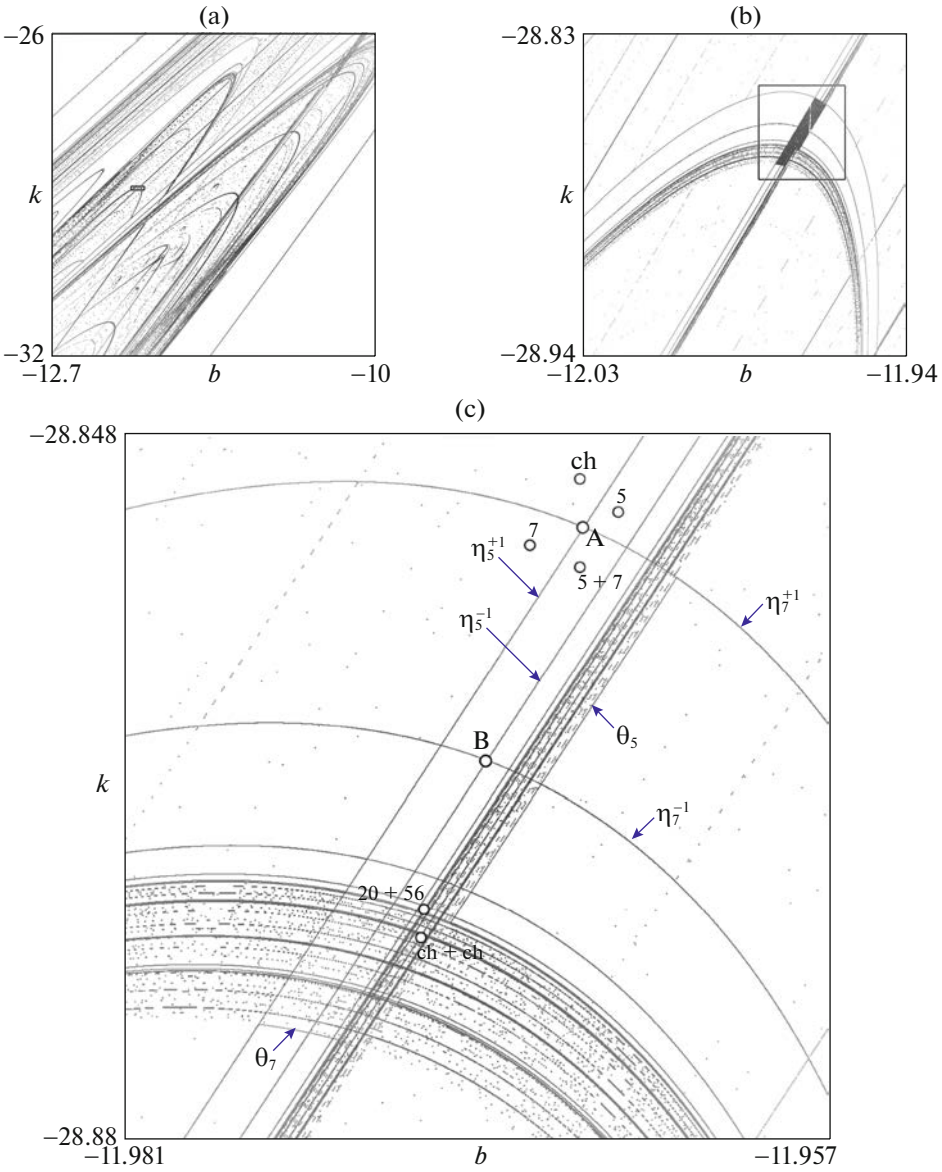

Fig. 5. Bifurcation structure in the (b, k) parameter plane. (a) Magnification of the rectangle marked in Fig. 4. (b) Magnification of the rectangle marked in (a). (c) Magnification of the rectangle marked in (b). Fold bifurcation curves η_5^{+1}, η_7^{+1}, flip bifurcation curves η_5^{-1}, η_7^{-1}, and final bifurcation curves θ_5, θ_7 are indicated. Attractors at the marked parameter points are shown in Figs. 6 and 7.

a countable set of curves associated with quasi-periodic dynamics (Feigenbaum-attractors) as well as by an uncountable set of curves related to non-robust chaotic dynamics. From the other side, the "tails", are confined by expansion or final bifurcations (see, e.g., [2]) of narrow-band chaotic attractors (interior and boundary crises, respectively) associated with homoclinic bifurcations of the unstable cycles appearing at the fold bifurcations.

It is well-known that such "tails" may overlap pairwise. In this case, two transversely intersecting fold bifurcation curves subdivide the parameter plane into four quadrants. In one of these quadrants, the attractors belonging to both overlapping "tails" coexist pairwise, which explains the occurrence of bistability in map (5). Accordingly, the region of bistability related to the intersection of two "tails" is confined by four bifurcation curves (two-fold bifurcations and two homoclinic bifurcations).

As an example, Fig. 5 presents a few subsequent magnifications of the bifurcation structure shown in Fig. 4. In particular, in Fig. 5c one can see the bifurcation structure close to the intersection point (marked by A) of the bifurcation curves η_5^{+1} and η_7^{+1} associated with fold bifurcations of 5- and 7-cycles,

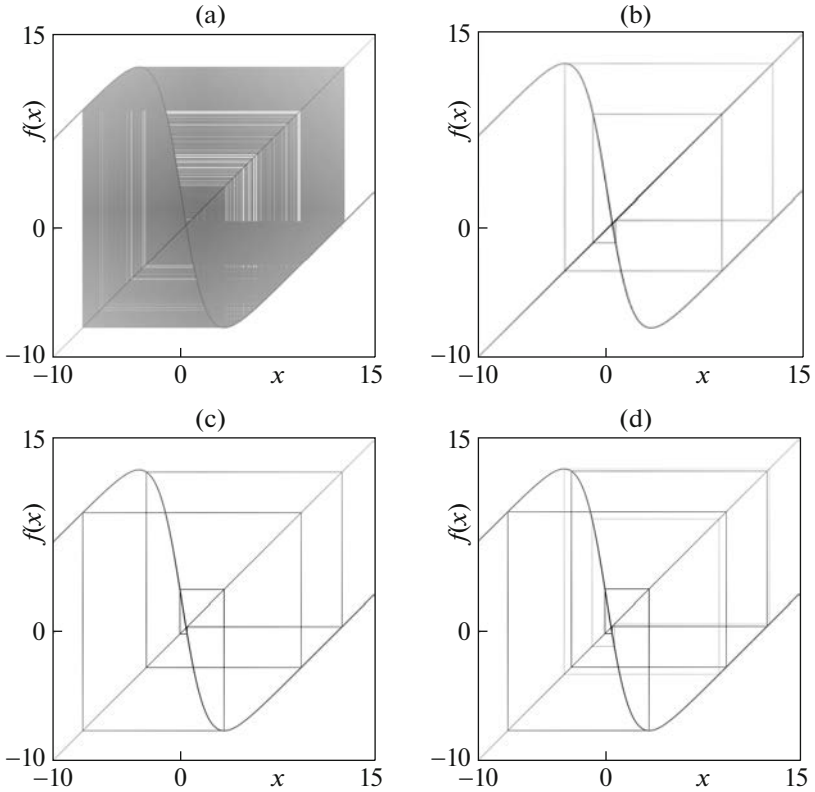

Fig. 6. Attractors of map (5) existing in the neighborhood of the intersection point of the fold bifurcation curves η_5^{+1} and η_7^{+1} (point A in Fig. 5c). (a) Unique broad-band chaotic attractor ($b = -11.9655$, $k = -28.85$); (b) unique 5-cycle ($b = -11.9642$, $k = -28.8515$); (c) unique 7-cycle ($b = -11.9672$, $k = -28.853$); (d) coexisting 5-cycle ($b = -11.9655$, $k = -28.854$).

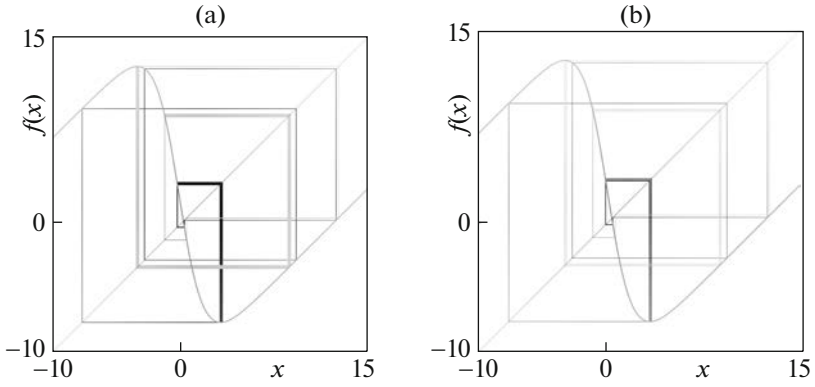

Fig. 7. Coexisting attractors of of map (5): (a) two narrow-band chaotic attractors ($b = -11.9709$, $k = -28.8708$); (b) a 20-cycle and a 56-cycle ($b = -11.9708$, $k = -28.8695$).

respectively. Examples of attractors of map (5) at parameter values belonging to a neighborhood of point A are shown in Fig. 6. As one can see, in the quadrant above this point (i.e., before the fold bifurcations occurring at η_5^{+1} and η_7^{+1}), the map has a unique broad-band chaotic attractor (see Fig. 5a). In the quadrant on the left of this point (i.e., before the fold bifurcation occurring at η_5^{+1} but after the fold bifurcation occurring at η_7^{+1}), the stable 7-cycle is the unique attractor (Fig. 6b). Similarly, in the quadrant on the right of point A (i.e., after the fold bifurcation occurring at η_5^{+1} but before the fold bifurcation occurring at η_7^{+1}), the unique attractor of the map is the stable 5-cycle (Fig. 6c). As for

the quadrant located below the point A (i.e., after both the fold bifurcations occurring at η_5^{+1} and η_7^{+1}), here the stable 7- and 5-cycles coexist (Fig. 6d).

At the bifurcation curves η_5^{-1} and η_7^{-1} the stable 5- and 7-cycles appearing at η_5^{-1} and η_7^{-1}, respectively, undergo flip (period-doubling) bifurcations. At the point (marked by B in Fig. 5c), these curves intersect so that in its neighborhood, one can observe not only the coexistence of stable 5- and 7-cycles (in the quadrant above this point) but also the coexistence of stable 5- and 14- (in the quadrant on the left of this point), 10- and 7- (in the quadrant on the right of this point), and 10- and 14-cycles (in the quadrant below this point).

Under further parameter variation, both period-doubling cascades proceed, followed by complete logistic map scenarios. As a consequence, an arbitrary attractor belonging to one of these scenarios may coexist with an arbitrary attractor belonging to another one. As an example, Fig. 7 shows a pair of coexisting narrow-band chaotic attractors and a pair of coexisting cycles of periods 20 and 56.

5. CONCLUSION

We considered a model of a two-predators-one-prey system. Previously, it was demonstrated that under certain assumptions the dynamics system can be represented by a one-dimensional bimodal map. In the present work, we explained the bifurcation structure in the 2D parameter space of this map. We identified the region in the parameter space associated with bounded dynamics. Then, we described the domains in the parameter space associated with different attractors. As we have shown, these sets overlap pairwise, leading to bistability.

ACKNOWLEDGMENTS

Authors dedicate the paper to the memory of Gennadiy Alexeevich Leonov.

FUNDING

Viktor Avrutin was supported by DFG, AV 111/2-2. Sergey Kryzhevich was supported by Gdańsk University of Technology by the DEC 14/2021/IDUB/I.1 grant under the Nobelium—"Excellence Initiative—Research University" program.

REFERENCES

1. J. Alebraheem and Y. Abu-Hasan, "Persistence of predators in a two predators- one prey model with non-periodic solution," Appl. Math. Sci. **6**, 943–956 (2012).
2. V. Avrutin, L. Gardini, I. Sushko, and F. Tramontana, *Continuous and Discontinuous Piecewise-Smooth One-dimensional Maps: Invariant Sets and Bifurcation Structures,* Vol. 95 of *Nonlinear Science, Series A* (World Scientific, Singapore, 2019).
3. Y. V. Bakhanova, A. O. Kazakov, and A. G. Korotkov, "Spiral chaos in Lotka–Volterra like models," Zh. Srednevolzh. Mat. Ob-va **19** (2), 13–24 (2017).
4. G. J. Butler and P. Waltman, "Bifurcation from a limit cycle in a two predator one prey ecosystem modeled on a chemostat," J. Math. Biol. **12**, 295–310 (1981).
5. R. Devaney, *An Introduction to Chaotic Dynamical Systems* (CRC, Boca Raton, FL, 2003).
6. O. Diekmann and M. Kirkilionis, "Population dynamics: A mathematical bird's eye view," in *Trends in Nonlinear Analysis,* Ed. by M. Kirkilionis, S. Krömker, R. Rannacher, and F. Tomi (Springer, Berlin, 2003).
7. B. Dubey and R. K. Upadhuyay, "Persistence and extinction of one-prey and two-predators system," Nonlin. Anal.: Model. Control **9**, 307–329 (2004).
8. T. Eirola, A. V. Osipov, and G. Söderbacka, "Chaotic regimes in a dynamical system of the type many predators one prey," Res. Reports A, No. 386 (Helsinki Univ. Technol., Helsinki, 1996).
9. T. Eirola, A. V. Osipov, and G. Söderbacka, "On the appearance of chaotic regimes in one dynamical system of type two predators—one prey," Actual Probl. Mod. Math., Boxitogorsk **1**, 39–70 (1996).
10. A. Farajzadeh, M. H. R. Doust, F. Haghighifar, and D. Baleanu, "The stability of Gauss model having one-prey-and-two-predators," Abstr. Appl. Anal. **2012**, 219640 (2012).
11. W. Façanha, B. Oldeman, and L. Glass, "Bifurcation structures in two-dimensional maps: The endoskeletons of shrimps," Phys. Lett. A **377**, 1264–1268 (2013).
12. J. Gallas, "Dissecting shrimps: Results for some one-dimensional physical models," Phys. A (Amsterdam, Neth.) **202**, 196–223 (1994).

13. V. Hadžiabdić, M. Mehuljić, and J. Bektešević, "Lotka–Volterra model with two predators and their prey," TEM J. **6**, 132–136 (2017).
14. C. S. Holling, "The components of predation as revealed by a study of small-mammal predation of the European pine sawfly," Can. Entomol. **91**, 293–320 (1959).
15. S. Hsu, "Limiting behaviour for competing species," SIAM J. Appl. Math. **34**, 760–763 (1978).
16. S. Hsu, S. Hubell, and P. Waltman, "Competing predators," SIAM J. Appl. Math. **35**, 617–625 (1978).
17. S. Hsu, S. Hubell, and P. Waltman, "A contribution to the theory of competing predators," Ecol. Monogr. **48**, 337–349 (1978).
18. J. Keener, "Oscillatory coexistence in the chemiostat: A codimension two unfolding," SIAM J. Appl. Math. **43**, 1005–1018 (1983).
19. M. Liu and P. S. Mandal, "Dynamical behavior of a one-prey two-predator model with random perturbations," Commun. Nonlin. Sci. Numer. Simul. **28**, 123–137 (2015).
20. M. C. Montano and B. Lisena, "A diffusive two predators-one prey model on periodically evolving domains," Math. Methods Appl. Sci. (2021, in press).
21. A. V. Osipov and G. Söderbacka, "Poincaré map construction for some classic two predators—one prey systems," Int. J. Bifurc. Chaos Appl. Sci. Eng. **27**, 1750116 (2017).
22. D. F. M. Oliveira, M. Robnik, and E. Leonel, "Shrimp-shape domains in a dissipative kicked rotator," Chaos **21**, 043122 (2011).
23. N. Samardzija and L. D. Greller, "Explosive route to chaos through a fractal torus in a generalized Lotka–Volterra model," Bull. Math. Biol. **50**, 465–491 (1988).
24. D. Savitri, A. Suryanto, W. Kusumawinahyu, and Abadi, "A dynamics behaviour of two predators and one prey interaction with competition between predators," IOP Conf. Ser.: Mater. Sci. Eng. **546**, 052069 (2019).
25. D. Singer, "Stable orbits and bifurcations of maps of the interval," SIAM J. Appl. Math. **35**, 260–267 (1978).
26. H. Smith, "The interaction of steady state and Hopf bifurcations in a two-predator-one-prey competition model," SIAM J. Appl. Math. **42**, 27–43 (1982).
27. G. J. Söderbacka and A. S. Petrov, "Review on the behaviour of a many predator—one prey system," Dinam. Sist. **9** (37), 273–288 (2019).
28. R. Stoop, S. Martignoli, P. Benner, and Y. Uwate, "Shrimps: Occurrence, scaling and relevance," Int. J. Bifurc. Chaos **22**, 1230032 (2012).
29. A. Wikan and Ø. Kristensen, "Prey-predator interactions in two and three species population models," Discrete Dyn. Nat. Soc. **2019**, 9543139 (2019).